Expansion of FRT Operation Range and Reduction of Grid Current Distortion for Grid-Tied Matrix Converter

Jun-ichi Itoh, Kyota Asai, Keisuke Kusaka, Satoshi Nagai
Department of Electrical, Electronics and Information Engineering
Nagaoka University of Technology
Nagaoka, Niigata, Japan
itoh@vos.nagaokaut.ac.jp, k_asai@stn.nagaokaut.ac.jp, kusaka@vos.nagaokaut.ac.jp, satoshi_nagai@stn.nagaokaut.ac.jp

***Abstract*— This paper proposes a fault-ride-through (FRT) control method to expand a FRT operation range for a grid-tied matrix converter. In the conventional method, the grid reactive current is limited because the generator q-axis current is circulated in only the generator side. Consequently, the matrix converter cannot satisfy the FRT requirements due to the limitation of the grid reactive current. On the other hand, the proposed method circulates the q-axis current between the generator side and the grid side in order to increase the grid reactive current. This increases the maximum grid reactive current by 14% as compared to that of the conventional method. As the experimental result, the proposed method expands the FRT operation range from 44 % to 100%, whereas a grid current with a low THD of 9.69% during the FRT operation is obtained.**

Keywords—matrix converter; fault ride through; generator; reactive current; three-phase voltage sag

I. INTRODUCTION

Nowadays, wind turbine systems, distributed power generation systems, and low-head hydropower systems have attracted many attentions as sustainable energy systems [1]. In these systems, fault-ride-through (FRT) requirements for the grid-tied converters are applied in many countries in order to avoid a power interruption in a large scale when only a local grid fault occurs [2]. A power converter for the grid-tied system employed must satisfy the FRT requirements as following: 1) the grid-tied converter needs to continue to operate during the grid voltage sag when the remaining voltage and its duration are within a limitation defined by the grid requirements; 2) a reactive current is delivered to the grid dependently on the remaining voltage. Furthermore, the grid-tied converter also requires the following capability aside from the FRT requirements: 3) the grid-tied converter has to maintain the generator torque during the grid voltage sag as same as that in the normal operation. In the wind turbine system, the generator torque needs to be maintained regardless of the grid state in order to avoid unexpected acceleration and vibration of the wind turbine [3]. Similarly, in the distributed power generation system and the low-head hydropower system, the generator cannot react to a quick torque disturbance caused by the grid voltage sag [4].

Meanwhile, a matrix converter has also attracted many attentions as a high-performance AC-AC converter [5-6]. The matrix converter is expected to achieve higher efficiency, smaller size and longer life-time compared to a conventional back-to-back (BTB) system. In previous works, grid-tied systems using the matrix converter for the wind turbine or the distributed power generation system have been reported [7]. However, generator terminal voltage of the grid connected matrix converter is forced to be lower during the grid voltage sag because the matrix converter is a step-down converter. Thus, the matrix converter cannot satisfy the FRT requirements.

Several literatures have discussed the FRT method for the matrix converter [8-11]. A conventional FRT control method for the matrix converter has been proposed to achieve 1) the stable FRT operation, 2) the grid reactive current control and 3) the generator torque control in the same time during the voltage sag [11]. The problem in the past work is that the grid current amplitude during the FRT operation is limited by 0.88 p.u of that during the normal operation, because the conventional FRT method circulates the generator q-axis current in only the generator side. Consequently, the matrix converter cannot satisfy the FRT conditions when the voltage sag of more than 44% of the normal grid voltage occurs in the grid.

This paper proposes an improved FRT control method to expand a FRT operation range for a grid-tied matrix converter. The q-axis current is flown into the snubber circuit and the d-axis current is flown into a voltage source inverter (VSI) of an indirect matrix converter (IMC). The original idea of this paper is that the proposed method circulates the q-axis current in snubber circuit at both the generator side and the grid side during the FRT operation in order to increase the grid current. The originality in this paper is that the proposed method achieves both the expansion of the FRT operation range and the reduction of the grid current distortion. In consequence, the grid reactive current is increased to 1.0 p.u. as compared to 0.88 p.u. of the conventional method. As a result, the range of the FRT operation becomes 100% in this paper. In addition, the proposed method also achieves the grid current control with low distortion by using two kinds of the VSI vectors when the VSI connects a current source rectifier.

This paper is organized as following; first the control strategy of the grid-tied matrix converter during the FRT operation is explained. Second, the control of the dq-axis current in the generator to increase the grid reactive current is explained. Finally, the effectiveness of the proposed method is confirmed by experiment.

II. Circuit configuration

Fig. 1 shows the matrix converter which is used as an interface converter between the power grid and the generator. During the voltage sag, the active power supplied from the generator to the grid becomes zero because only the reactive current is flown to the grid. However, the same torque of the generator should be maintained as same as that before the voltage sag. Therefore, a brake system consisting of an IGBT and a braking resistor is employed in order to absorb the active power provided from the generator. In particular, the IGBT in the brake circuit is turned on during the voltage sag and the active power provided from the generator is consumed by the braking resistor R_{brk}. Note that this braking circuit is required not only in the system employing the matrix converter but also in the conventional BTB system. Hence, the advantages of the matrix converter compared to the conventional BTB system does not degrade. In the conventional method, the snubber circuit is only connected the generator side in order to prevent the grid active current from circulating. On the other hand, in the proposed method, the snubber circuit is connected in both the generator side and the grid side because the proposed method circulates the q-axis current in snubber circuit at both the generator side and the grid side.

III. Fault-ride-through control method for grid-tied matrix converter

Fig. 2 shows a circuit diagram of an indirect matrix converter (IMC) which is used to employ the proposed FRT control method. The modulation method for the matrix converter during the voltage sag uses a virtual indirect control method [5]. The virtual indirect control treats the matrix converter illustrated in Fig. 1 as the IMC which consists of a current source rectifier (CSR) and the voltage source inverter (VSI). This replacement simplifies a consideration about the modulation method during the voltage sag. Note that the LC filters is eliminated and the snubber circuit is composed of a diode bridge and a DC voltage source in Fig. 2. Then, in order to yield the same waveforms between the matrix converter and the IMC at the input and output terminals excluding an effect of the LC filter in Fig. 1, (1) should be satisfied.

$$\begin{bmatrix} s_{ru} & s_{su} & s_{tu} \\ s_{rv} & s_{sv} & s_{tv} \\ s_{rw} & s_{sw} & s_{tw} \end{bmatrix} = \begin{bmatrix} s_{up} & s_{un} \\ s_{vp} & s_{vn} \\ s_{wp} & s_{wn} \end{bmatrix} \begin{bmatrix} s_{rp} & s_{sp} & s_{tp} \\ s_{rn} & s_{sn} & s_{tn} \end{bmatrix} \tag{1}$$

Fig. 3 shows a modulation block diagram of the matrix converter for the FRT operation. A single-phase modulation is employed to the CSR in order to modify the grid power factor reference during the voltage sag [5]. This results in the same modulation scheme of the CSR in both the grid normal operation and the voltage sag. On the other hand, the VSI has to change the modulation strategy in response to the grid state.

Fig. 4 shows the operation of the VSI in the voltage sag. In the conventional method, the matrix converter cannot satisfy the FRT requirements due to the limitation of the grid reactive current. Therefore, in the proposed method, the grid reactive current is increased by flowing the q-axis current in snubber circuit from the generator side to the grid side. In order to increase the grid reactive current, the control of the matrix converter is separated into three modes; a) the generator power factor control mode (only one phase is open), b) the DC-link conduction mode, and c) the freewheeling mode. In a) the

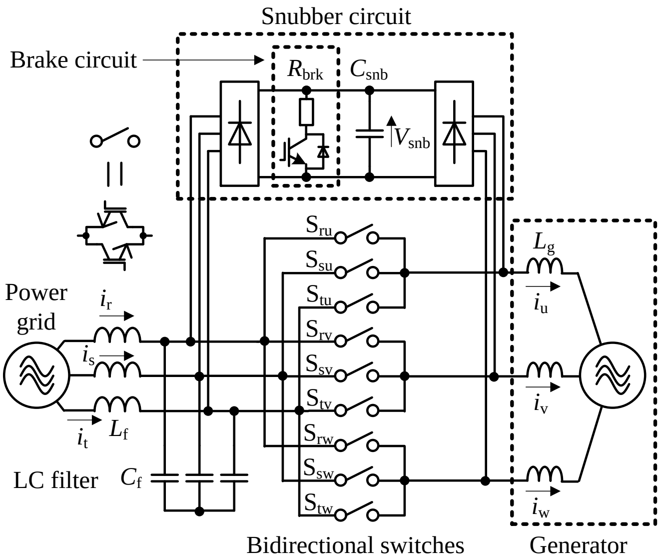

Fig.1. Circuit configuration of a matrix converter.

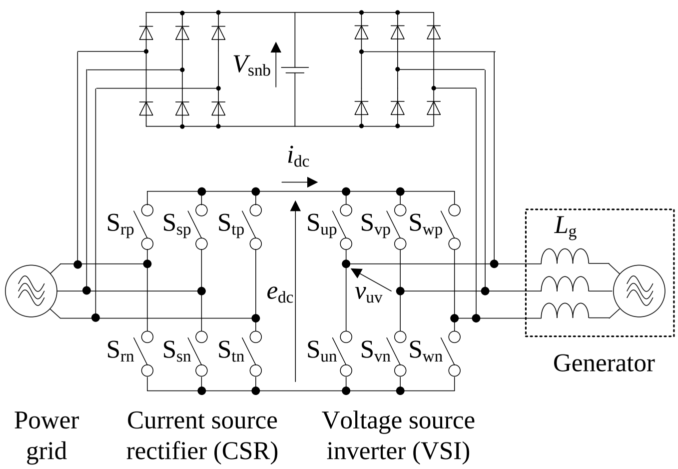

Fig.2. Circuit diagram of indirect matrix converter.

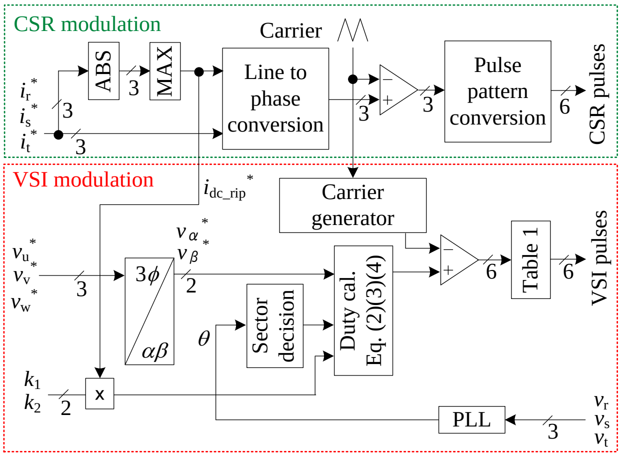

Fig.3. Modulation block diagram in FRT mode.

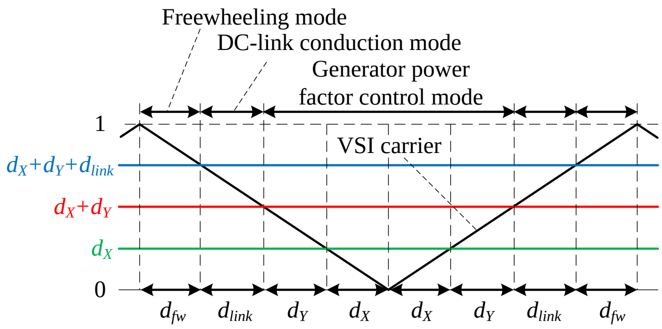

Fig.4. VSI operation in short voltage sag.

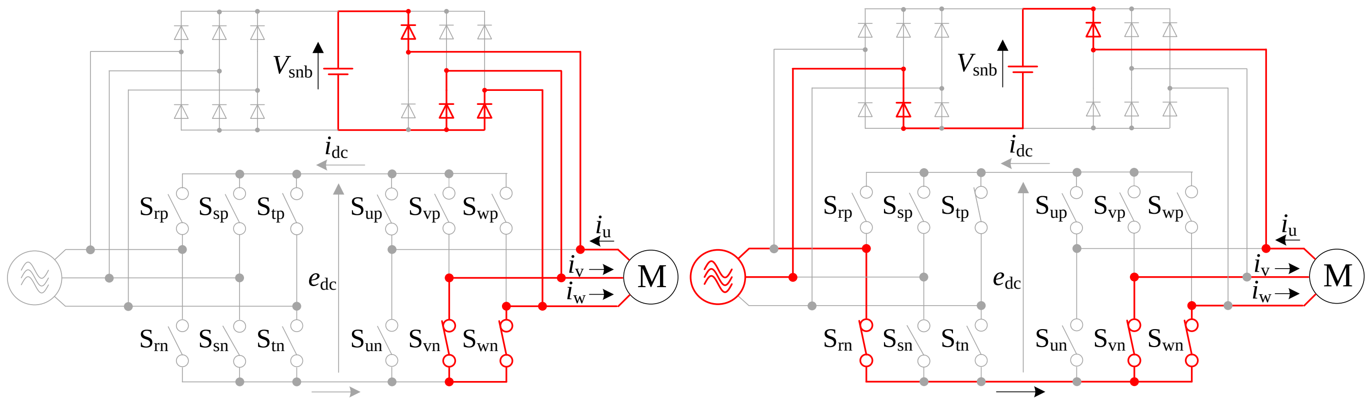

(a) In conventional method, active q-axis current circulates only in snubber circuit at generator side.

(b) In proposed method, q-axis current is controlled in order to circulate between generator side and grid side.

Fig.5. Current path in generator power factor control mode.

generator power factor control mode, the dq-axis currents of the generator are controlled. In b) the DC-link conduction mode, the VSI and the CSR are connected in order to let the grid reactive current circulate in the matrix converter. On the other hand, c) the freewheeling mode let the reactive current circulate only in the VSI.

A. Mode 1: Generator power factor control mode

Fig. 5 shows the current path in the generator power factor control mode. In this mode, the q-axis current is flown into the snubber circuit and the reactive d-axis current is flown into the IMC. In the conventional FRT method, the active q-axis current circulates only in snubber circuit at the generator side. On the other words, the grid reactive current in the conventional method is always zero. Consequently, the matrix converter cannot satisfy the FRT requirements for the grid reactive current. On the other hand, in the proposed method, instead of let q-axis current circulate only in the generator-side snubber circuit, the q-axis current is controlled in order to circulate between the generator side and the grid side. This enables the increase of the grid reactive current.

Table I shows the VSI pulse generation based on the conduction states of the diode rectifier during the generator power factor control mode. By selecting the short-circuit pathway of the generator, the current direction flow into the diode rectifier and the generator voltages are controlled, i.e. the control of the dq-axis currents. In particular, the conduction states of the diode rectifier define six space vectors from V1 to V6. The VSI controls the generator power factor by a current regulator (ACR) as following; two vectors from V1 to V6 which are adjacent to the voltage references v_α^*, v_β^* are selected. Then the duties d_X , d_Y of the output voltage vector v_X , v_Y are expressed by (2) and (3) based on these two selected vectors.

$$d_X = \left|v_\alpha v_{Y\beta} - v_{Y\alpha} v_\beta\right| / \left|v_{X\alpha} v_{Y\beta} - v_{Y\alpha} v_{X\beta}\right| \tag{2}$$

Table I. Virtual VSI pulse table.

Conduction state of diode rectifier $[D_u, D_v, D_p]$	VSI pulse (S_u, S_v, S_w)	Conduction state of diode rectifier $[D_u, D_v, D_p]$	VSI pulse (S_u, S_v, S_w)
V1 [1 0 0]	(X 0 0)	V4 [0 1 1]	(X 1 1)
V2 [1 1 0]	(1 1 X)	V5 [0 0 1]	(0 0 X)
V3 [0 1 0]	(0 X 0)	V6 [1 0 1]	(1 X 1)

Note: 1:Upper arm (D_{xp}, S_{xp}) ON 0:Lower arm (D_{xn}, S_{xn}) ON X:OPEN
x = u,v,w

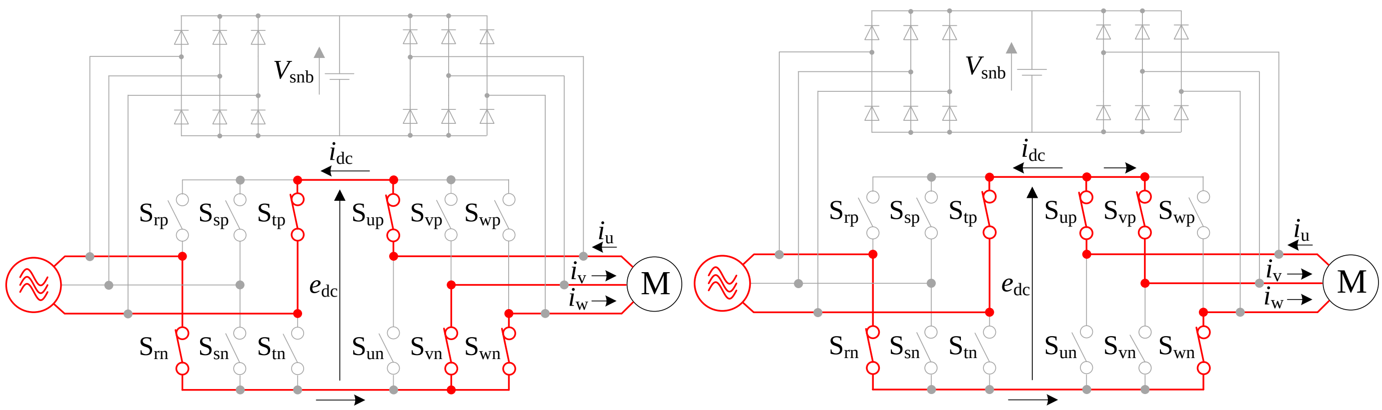

(a) All generator current injects to virtual DC-link. (b) Part of generator current circulates at virtual VSI.

Fig.6. Current path in DC-link conduction mode.

$$d_Y = \left|v_{X\alpha} v_\beta - v_\alpha v_{X\beta}\right| / \left|v_{X\alpha} v_{Y\beta} - v_{Y\alpha} v_{X\beta}\right| \tag{3}$$

B. Mode 2: DC-link conduction mode

Fig. 6 shows the current path in the dc-link conduction mode. During the off-state period of the diode bridge rectifier, the VSI outputs the vector based on the conduction states of the diode bridge rectifier, which is selected by the generator power factor control mode. In particular, the VSI outputs the vector based on the ratio between the duties d_X, d_Y and the sum of d_X, d_Y. In Fig. 6(a), the dc-link current i_{dc} becomes the u-phase current i_u. This switching pattern achieves the maximum i_{dc}. However, i_{dc} depends on the generator current, and the matrix converter is not control the grid current to the sinusoidal waveform. Therefore, in the generator current same as Fig. 6(a), the VSI outputs the switching pattern of Fig. 6(b) instead. Consequently, a part of the generator current circulates in the VSI. Due to this operation, i_{dc} is obtained by two kinds of the VSI vectors of the generator current independently. In this mode, the average voltage of the dc-link is zero every 1/6 of the grid period. In conclusion, by this mode, the constant dc-link current is obtained and the generator terminal voltage equals to the dc-link voltage, because all phases of the generator side are connected to the dc-link. This mode is controlled by the dc-link conduction duty d_{link} expressed by (4).

$$d_{link} = (k_1 + k_2)(1 - d_X - d_Y) * i_{dc\_rip}^{*} \tag{4}$$

where k_1 and k_2 are the ratio between the duties d_X ,d_Y and the sum of d_X , d_Y. Note that the multiplication of $i_{dc\_rip}^{*}$ is to match the ripple of i_{dc} to the frequency of the grid current and to control the grid current to sinusoidal waveform. The value of k_1, k_2 are expressed by (5) and (6).

$$k_1 = d_X / (d_X + d_Y) \tag{5}$$

$$k_2 = d_Y / (d_X + d_Y) \tag{6}$$

C. Mode 3: Freewheeling mode

Fig. 7 shows a current path in the freewheeling mode. In this mode, a zero vector is chosen to obtain a circulating path for the generator current. Consequently, the dc-link voltage and the generator terminal voltage become zero. This mode is controlled by the freewheeling duty d_{fw} expressed by (7).

$$d_{fw} = 1 - d_X - d_Y - d_{link} \tag{7}$$

IV. Feedback Controls during Voltage Sag

Fig. 8 shows a feedback control block diagram for the FRT operation. As shown in Fig. 1, it is required to control the snubber voltage and the generator current stably during the voltage sag in order to obtain a stable FRT operation and a desired generator torque. Hence, this paper uses two feedback controls for the snubber voltage and the generator current. In particular, the snubber voltage control is defined as an outer loop and the generator current control is set as an inner loop. When the braking IGBT is turned on during the voltage sag, the snubber voltage reference V_{snb}^* is determined according to the active power consumed by the braking resistor R_{brk}, which is equivalent to control the generator torque. On the other hand, inner loop controls the generator dq-axis current according to the voltage sag. PI controllers are employed in to the snubber voltage and the generator current controls. By introducing these feedback controls, the stable FRT operation and the generator torque control are achieved during the voltage sag.

V. Simulation Results

Table II and III show simulation conditions and control parameters. This session presents simulation results using the circuit depicted in Fig. 1 to confirm the FRT capability, the grid reactive current and the generator torque controls with the proposed FRT method. Note that inductors and an AC voltage source are used instead of the generator and q-axis current of the inductors is evaluated as the generator torque in simulation. The voltage sag amplitude is set to 100%, i.e. the remaining voltage of 0%. Note that, during the voltage sag, the power factor of the generator is limited from 1 to cos $\pi/6$ due to the operation of the diode bridge rectifier. Therefore, in the proposed method, in order to output the maximum grid reactive current, the d-axis current of the generator is regulated at the limitation of the power factor of the generator, i.e. cos $\pi/6$.

Fig. 9 shows the simulation results of the matrix converter during the FRT operation under the ideal condition (ideal commutation and no delay of the voltage dip detection). The red waveforms of the generator terminal voltage (U-V) in Fig. 9 show the averaged waveforms by using a low pass filter with a cut-off frequency of 1 kHz. In Fig. 9, the voltage sag of 100% occurs and the matrix converter operates with the proposed FRT method during this period. During the FRT operation, the grid active current is reduced to almost zero and the grid reactive current is generated by the zero power factor modulation of the virtual CSR and the DC-link conduction mode of the virtual VSI. The grid current, the generator terminal voltage (U-V) and the generator current during the voltage sag are sinusoidal waveform, whereas the grid current THD is 5.84%. Note that the q-axis current during the voltage sag is kept to 1 p.u. during both the normal state and the FRT operation. This results in the constant generator power of 1500 W, i.e. the constant generator torque. On the other hand, the proposed method increases the d-axis current of the generator

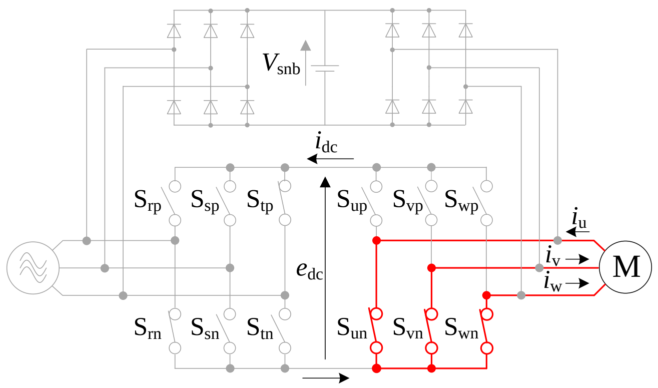

Fig.7. Current path in freewheeling mode.

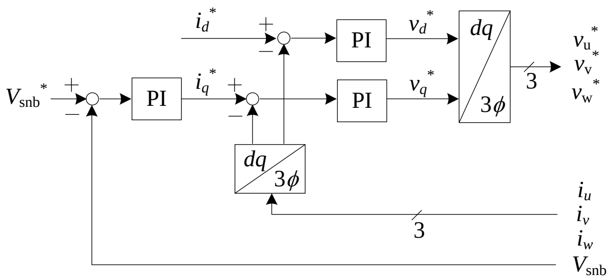

Fig. 8 Feedback control block diagram for FRT operation.

Table II Conditions of simulation and experiment.

Input line voltage	200 V	FRT duration	100 ms
Rated power	1500 W	Carrier frequency	10 kHz
Snubber capacitor	150 μF	Brake resistor	110 Ω
Grid side filter L (L_f)	2.15 mH (2.53%)	Generator back e.m.f.	140 V
Grid side filter C (C_f)	6.60 μF (5.54%)	Generator inductance (L_g)	3.86 mH (9.28%)

Table III Feedback control parameters.

Normal mode (Field oriented control)		d-axis current reference	0 p.u.
		q-axis current reference	-1.0 p.u.
		Proportional gain	1.2 p.u.
		Integral time	26.6 ms
FRT mode	Snubber voltage control	Voltage reference	400 V
		Proportional gain	2.0 p.u.
		Integral time	16.5 ms
	Generator current control	d-axis current reference	-0.577 p.u.
		Proportional gain	1.2 p.u.
		Integral time	1.65 ms

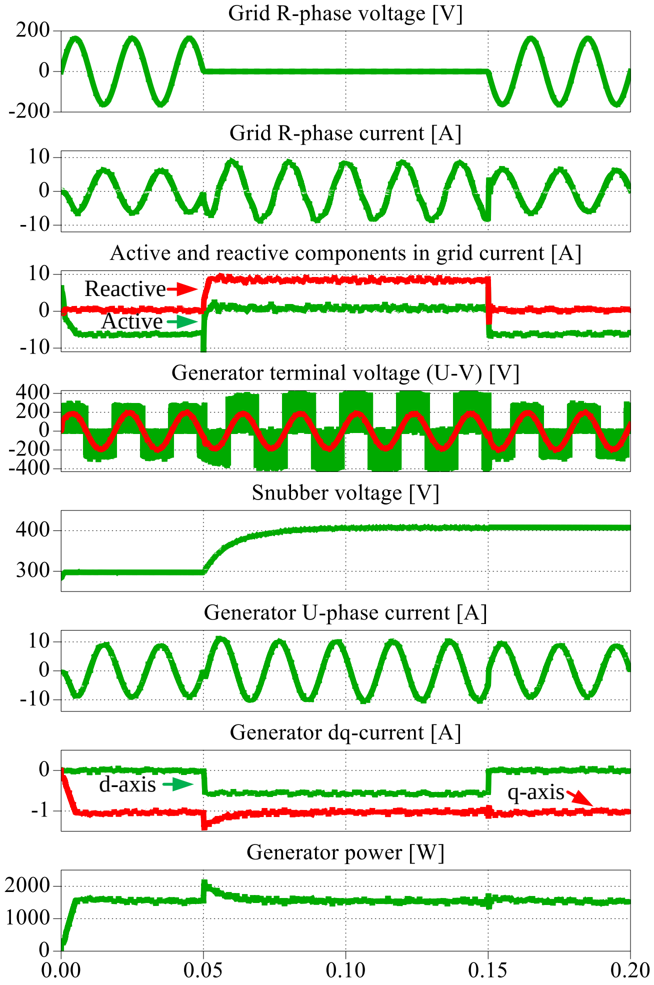

Fig. 9 Simulation results.

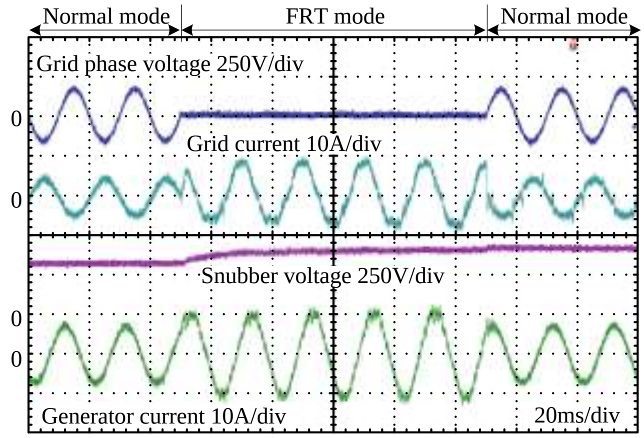

Fig.10 Operation waveform.

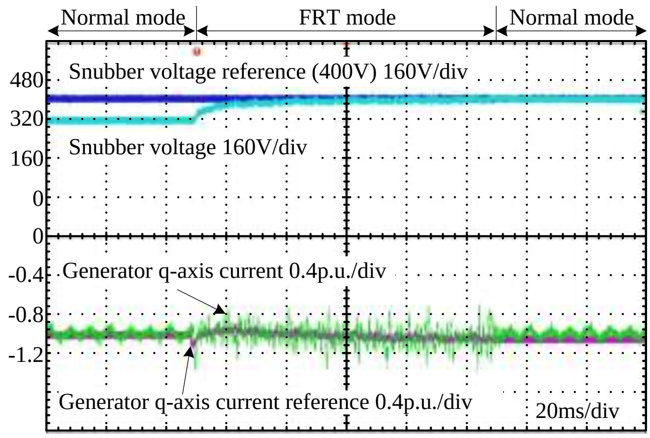

Fig.11 Responses of snubber voltage and generator q-axis current.

in order to obtain the power factor cos $\pi/6$, i.e. the condition to achieve the maximum grid reactive current. Therefore, the expansion of the FRT operation range is achieved by the proposed control.

VI. Experimental Results

Table II shows experimental conditions. This session presents experimental results using a prototype depicted in Fig. 1 to confirm the FRT capability, the grid reactive current and the generator torque controls with the proposed FRT method. Note that inductors and an AC voltage source are used instead of the generator and q-axis current of the inductors is evaluated as the generator torque in experiments. The voltage sag amplitude is set to 100%, i.e. the remaining voltage of 0%. Note that, during the voltage sag, the power factor of the generator is limited from 1 to cos $\pi/6$ due to the operation of the diode bridge rectifier. Therefore, in the proposed method, in order to output the maximum grid reactive current, the d-axis current of the generator is regulated at the limitation of the power factor of the generator, i.e. cos $\pi/6$.

Fig. 10 shows the operation waveform of the matrix converter during the three-phase voltage sag. In Fig. 5, the voltage sag of 100% occurs and the matrix converter operates with the proposed FRT method during this period. During the FRT operation, the grid active current is reduced to almost zero and the grid reactive current is generated by the proposed control method. The grid current and the generator current during the voltage sag are sinusoidal, whereas the grid current THD is 9.69%.

Fig. 11 shows the responses of the snubber voltage and the generator q-axis current. The snubber voltage reference is set to 400 V in order to obtain the same generator torque as before the voltage sag by using the braking resistor. As shown in Fig. 12, the snubber voltage and the generator q-axis current follow their references. As a result, a stable FRT operation is confirmed by the proposed control.

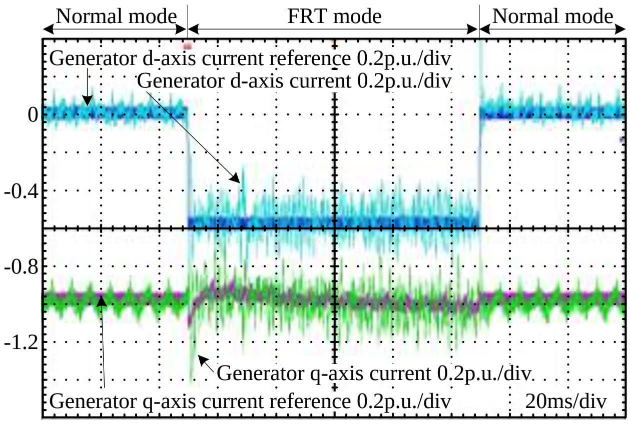

Fig.12 Generator dq-current response.

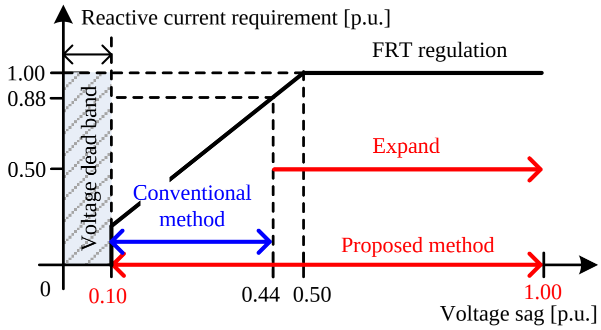

Fig.13 Relationship between voltage sag and reactive current requirement.

Fig. 12 shows the dq-axis current responses of the generator. The q-axis current reference during the voltage sag are kept to 1 p.u. in both the normal mode and the FRT operation in order to maintain the constant torque of the generator. As mentioned above, the active power generated from the generator during the FRT operation is transferred to the braking circuit by setting the snubber voltage reference to 400 V. Consequently, it is confirmed that the proposed FRT method obtains the same generator torque as before the voltage sag. Note that the ripple component in the dq-axis currents is caused by a zero-phase voltage fluctuation due to a two-phase modulation. On the other hand, the proposed method increases the generator d-axis current of 0.577 p.u. in order to obtain the power factor cos $\pi/6$, i.e. the condition to achieve the maximum grid reactive current. The effectiveness of the proposed control method in the experiments is confirmed as same as the simulation. In particular, the proposed method expands the FRT operation range for the grid-tied matrix converter.

Fig. 13 shows the relationship between the voltage sag and the reactive current requirement. The FRT operation is not applied in the voltage dead band, when the grid voltage sag is below 10% of the nominal value of the grid voltage. According to the grid requirements, the reactive current needs to be injected by 0.02 p.u. in response to each 1% of the grid voltage sag. The applicable range of the conventional FRT method is 44% or less, whereas the applicable range of the proposed method is extended to 100%.

VII. Conclusion

This paper proposed the FRT method for the grid-tied matrix converter in order to expand the FRT range. The proposed method circulated the q-axis current in the snubber circuit at both the generator side and the grid side during the FRT operation. This increased the grid reactive current, which expanded the FRT range. It was confirmed from the experimental result that the proposed method achieved the stable FRT operation during the voltage sag of 100%. Furthermore, the maximum value of the grid reactive current was increased by 14% as compared to that of the conventional method. Consequently, the range of the FRT operation was expanded from 44 % or less to 100%.

References

[1] S. Y. R. Hui, W. Zhong, C. K. Lee: "A Critical Review of Recent Progress in Mid-Range Wireless Power Transfer", IEEE Trans. On Power Electronics, Vol. 29, No. 9, pp. 4500-4511 (2014)

[2] S. Li, C. C. Mi: "Wireless Power Transfer for Electric Vehicle Applications", IEEE Journal of Emerging and Selected Topics in Power Electronics, Vol. 3, No. 1, pp. 4-17 (2015)

[3] D. Shimode, T. Murai, S. Fujiwara, "A Study of Structure of Inductive Power Transfer Coil for Railway Vehicles", IEEJ Journal of Industry Applications, Vol. 4, No. 5, pp. 550-558 (2015).

[4] R. Ota, N. Hoshi, and J. Haruna, "Design of Compensation Capacitor in S/P Topology of Inductive Power Transfer System with Buck or Boost Converter on Secondary Side", IEEJ Journal of Industry Applications, Vol. 4, No. 4, pp. 476-485 (2015)

[5] H. Ishida, H. Furukawa, T. Kyoden, "Development of Design Methodology for 60Hz Wireless Power Transmission System", IEEJ Journal of Industry Applications, Vol. 5, No. 6, pp. 429–438 (2016)

[6] K. Kusaka, K. Orikawa, J. Itoh, I. Hasegawa, K. Morita, T. Kondo, "Galvanic Isolation System with Wireless Power Transfer for Multiple Gate Driver Supplies of a Medium-voltage Inverter," IEEJ Journal of Industry Applications, Vol. 5, No. 3, pp. 206–214 (2016)

[7] N. K. Trung, T. Ogata, S. Tanaka, K. Akatsu, "Analysis and PCB Design of Class D Inverter for Wireless Power Transfer Systems Operating at 13.56MHz", IEEJ Journal of Industry Applications, Vol. 4, No. 6, pp. 703-713 (2015)

[8] M. Jo, Y. Sato, Y. Kaneko, S. Abe: "Methods for Reducing Leakage Electric Field of a Wireless Power Transfer System for Electric Vehicles", IEEE Energy Conversion Congress and Exposition (ECCE) 2014, pp.1762-1769 (2014)

[9] H. Kim, J. Cho, S. Ahn, J. Kim, J. Kim: "Suppression of Leakage Magnetic Field from a Wireless Power Transfer System using Ferrimagnetic Material and Metallic Shielding", IEEE International Symposium on EMC, 978-1-4673-2061-0, pp.640-645 (2012)

[10] T. Campi, S. Cruciani, M. Feliziani: "Magnetic Shielding of Wireless Power Transfer Systems", IEEE International Symposium on EMC, 15A-H1, pp.422-425 (2014)

[11] K. Maikawa, K. Imai, Y. Minagawa, M. Arimitsu, H. Iwao: "Magnetic Field Reduction Technology of Wireless Charging System", in

Proceedings, Society of Automotive Engineers of Japan 2013, No. 110-13 (2013)

[12] T. Shijo, K. Ogawa, M. Suzuki, Y. Kanekiyo, M. Ishida, S. Obayashi, "EMI Reduction Technology in 85 kHz Band 44 kW Wireless Power Transfer System for Rapid Contactless Charging of Electric Bus", IEEE Energy Conversion Congress & Expo 2016, No. EC-0641 (2016)

[13] K. Inoue, K. Kusaka, J. Itoh, "Reduction on radiation noise level for inductive power transfer systems with spread spectrum focusing on combined impedance of coils and capacitors," IEEE Energy Conversion Congress and Exposition (ECCE) 2016, pp. 1-8 (2016)

[14] K. Inoue, K. Kusaka, J. Itoh, "Reduction in Radiation Noise Level for Inductive Power Transfer Systems using Spread Spectrum Techniques," IEEE Trans. on Power Electronics, Vol. PP, No. 99, pp. 1-1 (2017)

[15] CISPR 11: 2015, "Industrial, scientific and medical equipment – Radio-frequency disturbance characteristics – Limits and methods of measurement (2015)

[16] Ministry of Internal Affairs and Communications, Japan, "Inquiry of technical requirements for wireless power transfer system for EVs in technical requirements for wireless power transfer system in standards of International Special Committee on Radio Interference (CISPR)", No. 3 (2015) (in Japanese)

[17] Y. H. Sohn, B. H. Choi, E. S. Lee, G. C. Lim, G. Cho, C. T. Rim: "General Unified Analyses of Two-Capacitor Inductive Power Transfer Systems: Equivalence of Current-Source SS and SP Compensations", IEEE Trans. On Power Electronics, Vol. 30, No. 11, pp. 6030-6045 (2015)

[18] R. Bosshard, J. W. Kolar, J. Muhlethaler, I. Stevanovic, B. Wunsch, F. Canales: "Modeling and eta-alpha-Pareto Optimization of Inductive Power Transfer Coils for Electric Vehicles", IEEE Journal of Emerging and Selected Topics in Power Electronics, Vol. 3, No. 1, pp. 50-64 (2015)

[19] R. L. Steigerwald, "A Comparison of Half-Bridge Resonant Converter Topologies," IEEE Trans. on Power Electronics Vol. 3, No. 2, pp. 174-182 (1992)

[20] K. Kim, Y. Jung, Y. Lim, "A New Hybrid Random PWM Scheme," IEEE Trans. on Power Electronics, Vol. 24, No. 1. pp. 192- 200 (2009)

[21] F. J. MacWilliams, N. J. A. Sloane, "Pseudo-random sequences and arrays," Proceedings of the IEEE, Vol. 64, No. 12, pp. 1715-1729 (1976)